

Rubidium 5^2P fine-structure transitions induced by collisions with potassium and caesium atoms

C Vadla, S Knezovic and M Movre

Institute of Physics of the University, 41001 Zagreb, POB 304, Croatia

Received 5 August 1991, in final form 21 October 1991

Abstract. A diode-laser fluorescence experiment was performed in order to study fine-structure transitions between 5^2P states of rubidium atoms colliding with ground-state potassium or caesium atoms. The $Rb(5^2P_{3/2})$ state was optically excited and the intensity ratio of sensitized to direct fluorescence was measured. The obtained cross sections for the excitation energy transfer $Rb(5^2P_{3/2}) \rightarrow Rb(5^2P_{1/2})$ induced by collisions with K and Cs ($T = 573$ K) are $\sigma = 54 \text{ \AA}^2 \pm 30\%$ and $\sigma = 15 \text{ \AA}^2 \pm 30\%$, respectively. Assuming detailed balancing, the cross sections for the reverse process $Rb(5^2P_{1/2}) \rightarrow Rb(5^2P_{3/2})$ are $\sigma = 60 \text{ \AA}^2 \pm 30\%$, and $\sigma = 16.5 \text{ \AA}^2 \pm 30\%$ for K and Cs, respectively.

1. Introduction

During the last decades excitation energy transfer processes in low-energy atomic collisions have been the subject of numerous experimental and theoretical papers. Among them collisionally induced transitions between the fine-structure components of the first excited alkali levels have drawn considerable attention. In most cases inert-gas atoms were perturbers, but there are a few experiments in which alkali atoms are the collision partners. There are significant discrepancies among experimental results of different groups and very often the theoretical cross sections are much smaller than the experimental values. The experimental and theoretical results in this field published up to 1975 are summarized by Krause (1975).

In the case of collisions between dissimilar alkali atoms, most of the work has been done in K–Rb mixtures. The mixing between the 4^2P states of a potassium atom, induced in a collision with a rubidium atom in the ground state has been studied experimentally by Hrycyshyn and Krause (1969a). The experiments were carried out at partial pressures of potassium vapour at which the imprisonment of resonance radiation may be disregarded. The excitation transfer from potassium 4^2P resonance states to rubidium 5^2P resonance states has been investigated by several authors (Thangaraj 1948, Hrycyshyn and Krause 1969b, Ornstein and Zare 1969, Stacey and Zare 1970). The experimental results differ considerably and there are no obvious reasons to account for the discrepancies (Krause 1975). The theoretical aspects of excitation transfer in K–Rb mixtures were considered by Dashevskaya *et al* (1969a, b).

The excitation transfer from rubidium 5^2P resonance states to caesium 6^2P resonance states have been studied by Czajkowski *et al* (1966). Their results, as well as some of those for K–Rb transfer (Hrycyshyn and Krause 1969b), have been found to fit very well into the general scheme of cross sections for inelastic collisions between dissimilar partners (Czajkowski *et al* 1973).

The present investigation is concerned with the excitation energy transfer between the fine-structure components of the rubidium atom in the 5^2P resonance state, induced by collisions with ground-state potassium or caesium atoms. The particular mixing process can be described by the following equation:



where ΔE , the energy defect between the $5^2P_{1/2}$ and $5^2P_{3/2}$ states of rubidium, equals 237.6 cm^{-1} , and M represents either K ($n=4$) or Cs ($n=6$). We are not aware of any previous study of these processes.

2. Experimental and method

Figure 1 shows a schematic diagram of the experimental set-up. High-purity alkali metal (K or Cs) with small amount of an inevitable Rb fraction was contained in the side-arm of a 120 mm long cylindrical cell, 28 mm in diameter, made of Pyrex glass. During the measurement the temperature of the cell was kept constant at 300°C while the side-arm temperature was changed in the range from 200°C to 280°C . The K (or Cs) number density was determined spectroscopically by the white-light absorption measurement (not displayed in figure 1) in the blue wing of the self-broadened resonance D2 line. The 1 m McPherson monochromator (slit width $10 \mu\text{m}$, band pass 0.01 nm) with the RCA S-20 multiplier was used. The rubidium atoms in K (or Cs) vapours were excited to the $5^2P_{3/2}$ state by a single-mode frequency stabilized diode laser (Mitsubishi MD series, wavelength 781.0 nm at 25°C , linewidth about 25 MHz , maximal power 5 mW). The laser beam passed through the cell perpendicular to the cell's cylindrical axis at a distance about 5 mm from the cell window. The cross section of the laser beam was about 1 mm^2 . Optical saturation was avoided by using neutral-density filters for the attenuation of the laser power (down to about 0.1 mW). In order to eliminate the laser light scattered from the cell walls, a mask having a 5 mm aperture was placed in the front of the cell window. The fluorescence zone was imaged onto the entrance slit of the monochromator at right angles to the laser beam direction. The

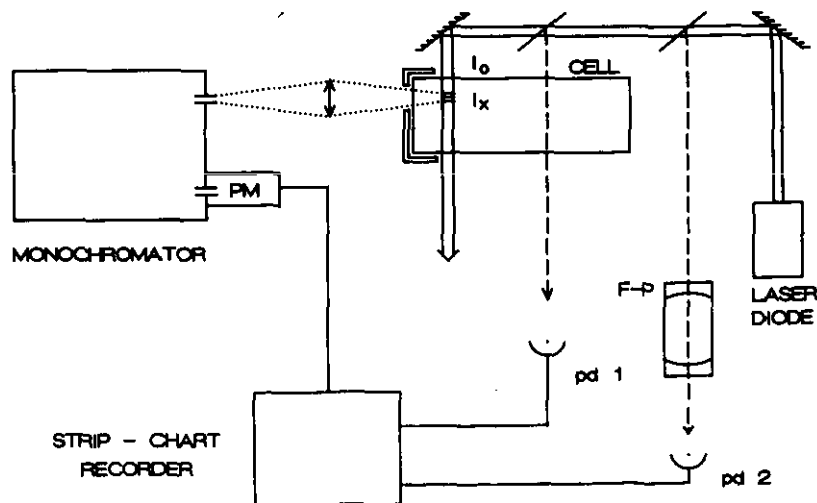


Figure 1. Experimental set-up.

broad-band adjusted monochromator (slit width $500\ \mu\text{m}$, band pass $0.5\ \text{nm}$) was tuned either to the Rb D2 or the Rb D1 line, while in both cases the laser was scanned over the Rb $5^2S_{1/2} \rightarrow 5^2P_{3/2}$ transition. In this manner, the spectrally unresolved resonant (I_2) or sensitized (I_1) fluorescence was measured versus laser frequency ν_L . The linearity of the laser scan was controlled using the $0.5\ \text{m}$ confocal Fabry-Perot interferometer. Typical spectra are shown in figure 2. As one can see, the spectra exhibit the known isotope and hyperfine structure of the Rb D2 line. The lines labelled as a, b, c and d correspond to collisionally and Doppler broadened transitions $^{87}\text{Rb } 5^2S_{1/2}(F=1) \rightarrow 5^2P_{3/2}(F')$, $^{87}\text{Rb } 5^2S_{1/2}(F=2) \rightarrow 5^2P_{3/2}(F')$, $^{85}\text{Rb } 5^2S_{1/2}(F=2) \rightarrow 5^2P_{3/2}(F')$, and $^{85}\text{Rb } 5^2S_{1/2}(F=3) \rightarrow 5^2P_{3/2}(F')$, respectively. Additionally, for control of the Rb number density and optical depth of the rubidium lines, the absorption of the laser beam along a $28\ \text{mm}$ optical path was recorded (see also figure 1).

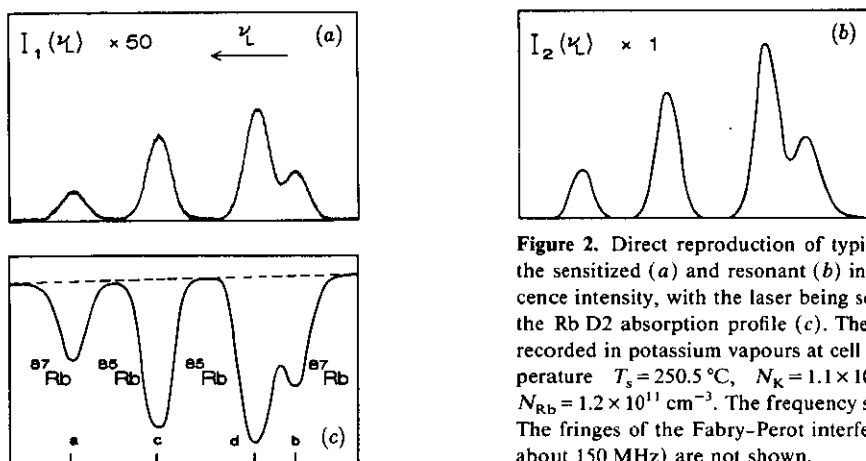


Figure 2. Direct reproduction of typical spectra of the sensitized (a) and resonant (b) integral fluorescence intensity, with the laser being scanned across the Rb D2 absorption profile (c). The spectra were recorded in potassium vapours at cell side-arm temperature $T_s = 250.5\ ^\circ\text{C}$, $N_K = 1.1 \times 10^{15}\ \text{cm}^{-3}$ and $N_{\text{Rb}} = 1.2 \times 10^{11}\ \text{cm}^{-3}$. The frequency scale is linear. The fringes of the Fabry-Perot interferometer (FSR about $150\ \text{MHz}$) are not shown.

In spite of the hyperfine splitting of the Rb levels and the existence of two stable isotopes, the evaluation of the obtained spectra was based upon a simple three-level model which includes the relevant transition rates. This approach was applied by many authors since Krause's pioneering work (Krause 1966) and it will be redone here with a few extensions concerning some specific points in our experiment.

Since the densities of K and Cs atoms were much larger than that of rubidium (about 10^4 and 6×10^4 times for K and Cs, respectively), the fine-structure mixing process $\text{Rb}(5^2P_{3/2}) \leftrightarrow \text{Rb}(5^2P_{1/2})$ was induced only due to collisions with K (or Cs). Therefore, this process can be treated separately for the ^{87}Rb and ^{85}Rb isotopes. For illustration, the partial energy-level diagram of the ^{87}Rb isotope ($I = \frac{3}{2}$, natural abundance 27.8%) together with the hyperfine splitting and relevant transition rates is shown in figure 3. Spontaneous emission rates for the Rb 5^2P fine-structure components are denoted by A . The average value for A taken from Hansen (1984) is $3.7 \times 10^7\ \text{s}^{-1}$. Fine-structure collisional mixing rates C and D are defined analogously to the gas kinetic rates as the product $\nu\sigma N_p$, where ν is the mean interatomic velocity, N_p is the density of atoms inducing the transfer and σ is the corresponding cross section.

For the sake of simplicity, we label the states $5^2S_{1/2}$, $5^2P_{1/2}$ and $5^2P_{3/2}$ as 0, 1 and 2, respectively. When state 2 is optically excited, the steady-state equation for the collisionally populated state 1 is

$$\dot{N}_1 = 0 = DN_2 - (A + C)N_1 \quad (1)$$

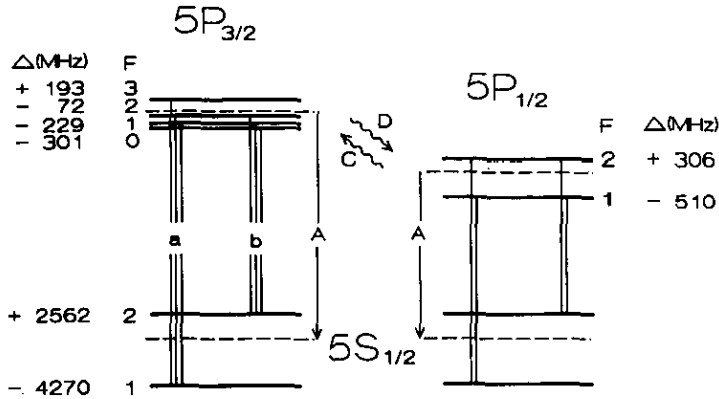


Figure 3. Partial term diagram for ⁸⁷Rb isotope with hyperfine energy splitting. A is the spontaneous emission coefficient of the Rb 5P state. The rates for collisional intermultiplet mixing within Rb 5P fine-structure levels are C and D.

which yields the population density ratio

$$N_1/N_2 = D/(A + C) \tag{2}$$

If the medium is optically thin, the sensitized-to-direct fluorescent intensity ratio I_1/I_2 equals N_1/N_2 . Using the principle of detailed balancing, which requires C and D to be in the ratio

$$\frac{C}{D} = \frac{g_2}{g_1} \exp[-(E_2 - E_1)/kT] \tag{3}$$

one can determine the rates C and D. Here g_i is the statistical weight and E_i the energy of the i th level.

The main problem and source of errors in many experiments dealing with the resonant fluorescence is the radiation trapping due to reabsorption in optical thick medium (Holstein 1947). This problem was usually solved by additional lifetime measurements (Huennekens and Gallagher 1983) or calculation of corrections (Kamke et al 1983). The trapping effect is very sensitive to the geometry of the experimental system and care must be exercised when calculating the corrections. In the present work, the radiation trapping was directly controlled during the measurements by comparing the sensitized-to-resonant fluorescence intensity ratios for pumping of different Rb D2 hyperfine components. Following the procedure and geometry of the present experiment we have applied this control mechanism in the following way. Let the laser beam of spectral intensity $I_0\delta(\nu - \nu_L)$ propagate in the x direction through the cell at a distance d from the cell window (see figure 1). When the laser frequency ν_L is tuned at the 0→2 transition, the power absorbed in the layer x, x + dx is

$$\begin{aligned} W_{0 \rightarrow 2}(x, \nu_L) &= \int d\nu I_x \delta(\nu - \nu_L) \alpha_2(\nu) s \, dx \\ &= I_x \alpha_2(\nu_L) s \, dx. \end{aligned} \tag{4}$$

Here $\alpha_2(\nu)$ is the classical absorption coefficient for the 0→2 transition, s is the laser beam cross section and I_x is the attenuated laser intensity at x, given by $I_x = I_0 \exp(-\alpha_2(\nu_L)x)$.

Level 1 is populated due to collisional excitation energy transfer, and the absorbed power will be spontaneously emitted in fractions of sensitized and resonant fluorescence:

$$h\nu_{10}N_1A_1 + h\nu_{20}N_2A_2 = W_{0\rightarrow 2}(x, \nu_L). \quad (5)$$

Here we assume the presence of radiation trapping, which manifests itself by decrease of the effective spontaneous emission rates having different values for states 1 and 2. Introducing the population density ratio $n_{12} = N_1/N_2 = D/(A_1 + C)$ into equation (5) and assuming $\nu_{10} \approx \nu_{20} = \nu$, we obtain the following expressions for spectral intensities of the sensitized and resonance fluorescence emitted from the infinitesimal volume $s \, dx$:

$$J_1(\nu) \propto P_1^E(\nu) \frac{n_{12}A_1}{n_{12}A_1 + A_2} W_{0\rightarrow 2}(x, \nu_L) \quad (6)$$

$$J_2(\nu) \propto P_2^E(\nu) \frac{A_2}{n_{12}A_1 + A_2} W_{0\rightarrow 2}(x, \nu_L). \quad (7)$$

Here $P_1^E(\nu)$ and $P_2^E(\nu)$ are the corresponding normalized emission profiles for the $1 \rightarrow 0$ and $2 \rightarrow 0$ transitions, respectively. Note that both the intensities follow the shape of the absorption coefficient α_2 when the laser is scanned across the $0 \rightarrow 2$ transition (see equation (4) and figure 2). The observed spectral intensities are distorted due to absorption on the path d between the fluorescence zone and the cell window. Here we suppose the radiation diffusion, which follows the effect of radiation trapping, to be negligible and accordingly the fluorescence zone to be restricted within the volume defined by the laser beam. If we denote the transmission of the medium for the Rb D1 and Rb D2 lines with $T_1(\nu, d)$ and $T_2(\nu, d)$, the ratio of the integral intensities, observed by using a broad-band detector, e.g., monochromator with wide slits, is given by

$$\frac{I_1}{I_2} = \frac{\int d\nu T_1(\nu, d) P_1^E(\nu) \frac{A_1}{A_2} \frac{D}{A_1 + C}}{\int d\nu T_2(\nu, d) P_2^E(\nu) \frac{A_2}{A_1 + C}}. \quad (8)$$

In the optically thin case ($T_1 = T_2 = 1$) and in the absence of radiation trapping ($A_1 = A_2 = A$) the ratio of the sensitized to direct fluorescence intensities should not depend on excitation channels, and equation (8) becomes

$$I_1/I_2 = D/(A + C). \quad (9)$$

Since the energy differences between the states 1 and 2 for both Rb isotopes are nearly equal, the transfer rates C and D should be practically the same for ^{87}Rb and ^{85}Rb . Therefore, in the case when the D1 and D2 lines of both isotopes are optically thin, one can expect that there will be no difference between the intensity ratios (9) when different isotopes are excited.

3. Data analysis and results

The ratios of the sensitized (Rb D1) to direct (Rb D2) fluorescence intensities were measured in K and Cs for laser frequencies tuned at the absorption maxima of the a, b, c and d hyperfine components of the ^{87}Rb and ^{85}Rb D2 lines. In figure 4 the values for $I_1(\alpha)/I_2(\alpha)$, i.e. the ratios of peak intensities for $\alpha = a, b, c$ and d , are plotted against the K (upper part) and Cs (lower part) number densities, respectively. Figure 5 shows the temperature dependence of the K atom density together with the density

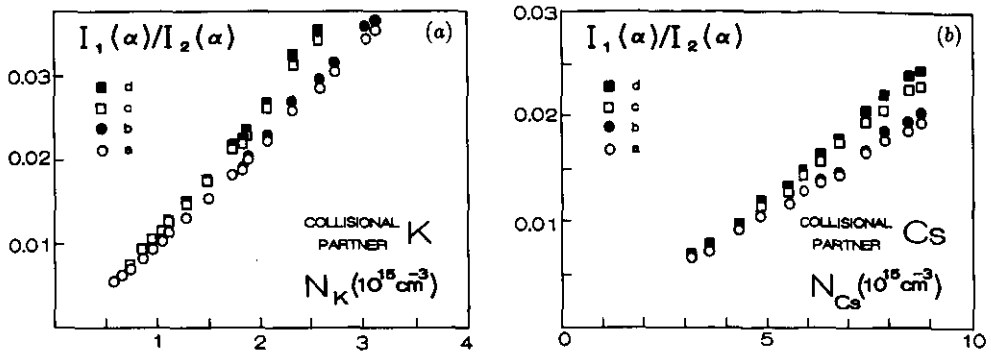


Figure 4. (a) Sensitized (Rb D1) to direct (Rb D2) fluorescence intensity ratios versus potassium number density. The ratios have been obtained for laser frequencies tuned at the absorption peaks of the ^{87}Rb D2 (a, b) and ^{85}Rb D2 (c, d) lines. (b) Analogous measurements in Cs vapours. The temperature T_c of the fluorescence cell was $(300 \pm 5)^\circ\text{C}$.

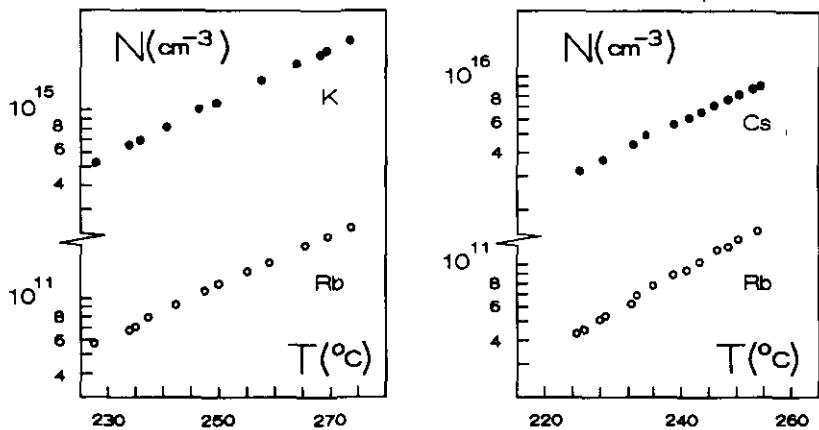


Figure 5. Potassium (left) and caesium number density (right) together with the density of the rubidium impurity plotted against the cell side-arm temperature T_c .

of the Rb impurity in K (left) and a similar diagram for Cs vapours (right). In both cases the Rb number density was measured by the laser absorption of the optically thin ^{87}Rb D2 component labelled by a. The value for the oscillator strength of this component is $\frac{3}{8}f(\text{Rb D2})$, where, as given by Hansen (1984), the total oscillator strength $f(\text{Rb D2})$ is 0.65. As mentioned in section 2, potassium and caesium number densities were determined by white-light absorption measurement in the blue wings of the self-broadened K D2 (766.5 nm) and Cs D2 (852.1 nm) lines, respectively. According to Beuc *et al* (1982), the potassium number density N_K is given by

$$N_K(\text{cm}^{-3}) = 2.83 \times 10^{16} \Delta\lambda(\text{nm})\sqrt{k(\text{cm}^{-1})}. \quad (10)$$

Here k is the absorption coefficient at a distance $\Delta\lambda$ from the line centre. The analogous formula used for Cs (Beuc *et al* 1982) is given by:

$$N_{\text{Cs}}(\text{cm}^{-3}) = 2.15 \times 10^{16} \Delta\lambda(\text{nm})\sqrt{k(\text{cm}^{-1})}. \quad (11)$$

As one can see in figure 4, the sensitized-to-direct fluorescent intensity ratios split due to radiation trapping into two groups, each for the corresponding isotope. Also the curves differ slightly for each particular isotope. For lower densities the radiation

trapping disappears and all curves become identical straight lines through the origin. This is the case for $N_K < 7 \times 10^{14} \text{ cm}^{-3}$ and $N_{Cs} < 3 \times 10^{15} \text{ cm}^{-3}$, i.e. when the Rb number density is lower than $6 \times 10^{10} \text{ cm}^{-3}$ (see figure 5). Since the fraction of the ^{87}Rb isotope is 2.6 times smaller than that of ^{85}Rb , one can conclude, with a great deal of certainty, that the curves $I_1(a)/I_2(a)$ have been measured in the absence of radiation trapping in as far as that the K and Cs densities were lower than $2 \times 10^{15} \text{ cm}^{-3}$ and $8 \times 10^{15} \text{ cm}^{-3}$, respectively. Therefore, the relation (9) can be applied for these curves. Since the intensity ratios $I_1(a)/I_2(a)$ are considerably smaller than unity, the rate C in the denominator can be neglected in comparison to the spontaneous emission rate A . Thus, using the data for $I_1(a)/I_2(a)$ the equation (9) gives directly rate D .

The calculated corresponding cross sections

$$\sigma_D = D/N_p \nu^{\text{Rb-X}}$$

for the processes $\text{Rb}(5^2P_{3/2}) + \text{K}(4^2S_{1/2}) \rightarrow \text{Rb}(5^2P_{1/2}) + \text{K}(4^2S_{1/2})$, and $\text{Rb}(5^2P_{3/2}) + \text{Cs}(6^2S_{3/2}) \rightarrow \text{Rb}(5^2P_{1/2}) + \text{Cs}(6^2S_{1/2})$ at the temperature $T = 573 \text{ K}$ ($\nu^{\text{Rb-K}} = 6.6 \times 10^4 \text{ cm s}^{-1}$, $\nu^{\text{Rb-Cs}} = 4.8 \times 10^4 \text{ cm s}^{-1}$) are

$$\sigma_D(\text{Rb}^* + \text{K}) = 54 \text{ \AA}^2$$

and

$$\sigma_D(\text{Rb}^* + \text{Cs}) = 15 \text{ \AA}^2$$

respectively. Assuming detailed balancing, the cross sections σ_C calculated using the equation (3) are

$$\sigma_C(\text{Rb}^* + \text{K}) = 60 \text{ \AA}^2$$

and

$$\sigma_C(\text{Rb}^* + \text{Cs}) = 16.5 \text{ \AA}^2.$$

The statistical accuracy of these data is about 5%, but the actual uncertainty is much greater due to the polarization effects. The collisionally populated Rb $5^2P_{1/2}$ state leads to unpolarized and isotropic D1 fluorescence. In contrast, the direct D2 fluorescence is partially polarized and anisotropic. Additionally, the Rayleigh scattering occurs at laser frequency ν_L . Thus, in this experiment the D2 signal has always been the sum of the polarized Rayleigh scattering and fluorescence. In principle, the contribution of Rayleigh scattering can be easily quantifiable by looking at intensities well off resonance. However, as described above, we did not spectrally resolve fluorescent light, but instead we have recorded the total intensity tuning the laser wavelength across the line. On the other hand, under present experimental conditions, the low intensity problem prevents a probe like this. A rough estimation of the polarization effects was done by placing a linear polarizer in front of the monochromator entrance slit. The ratios of the Rb D1 to D2 fluorescent intensities were measured for the directly excited component of the ^{87}Rb D2 line in potassium. The polarization of the laser beam was in the plane defined by the laser beam direction and the direction of observation. The measurements were performed for three different orientations of the polarizer with respect to the incident laser beam direction. The results are shown in figure 6. It can be seen that the variations among intensity ratios $I_1(a)/I_2(a)$ obtained for different orientations of the polarizer are about 40% in the case of the lowest potassium density. In the case of the highest potassium density the variations are smaller (about 20%). This is due to the fact that the impact broadening of the spectral lines destroys the polarization. If the impact broadening contribution to the Lorentzian linewidth Γ_{br} is much greater than the natural radiation broadening constant Γ_{nat} , the redistributed

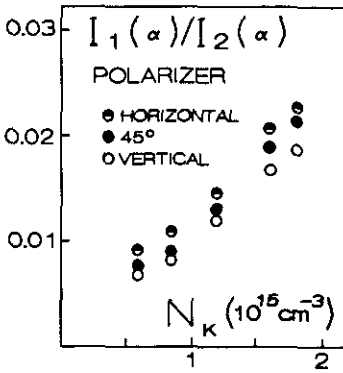


Figure 6. Sensitized ($^{87}\text{Rb D1}$) to direct ($^{87}\text{Rb D2}$) fluorescence intensity ratios in K plotted against the potassium density for various orientations of the polarizer placed in front of the monochromator entrance slit.

unpolarized and isotropic fluorescence dominates over the Rayleigh scattering (Ballagh and Cooper 1977). The impact broadening parameters relevant in the present work can be derived from the calculations of van der Waals interaction potentials for dissimilar alkali atoms (Movre and Beuc 1985).

For the Rb D2 line broadened by potassium, we have obtained the impact broadening parameter $\gamma_{\text{Rb-K}} = 6.2 \times 10^{-9} \text{ s}^{-1} \text{ cm}^3$, whereas in the case of Cs as the collisional partner, $\gamma_{\text{Rb-Cs}}$ has been found to be $2.8 \times 10^{-9} \text{ s}^{-1} \text{ cm}^3$. Thus, the contributions to the Lorentzian linewidth $\Gamma_{\text{br}} = N_X \gamma_{\text{Rb-X}}$ for the highest number densities of K and Cs in this experiment are 18.6 MHz and 25.2 MHz, respectively. Comparing these values with natural radiation broadening width for the Rb D2 ($\Gamma_{\text{nat}} = A/2\pi = 5.9 \text{ MHz}$) and using the results of Ballagh and Cooper (1977), we have estimated the systematic error due to polarization effects to be about $\pm 25\%$.

For evaluation of the scattering cross sections we used an average value of A coefficient. The best theoretical results (Hansen 1984, Theodosiu 1984) give the A coefficient for D2 transition about 6% higher than for D1 transition, and the differences among various experimental results are in the range of 10% (Theodosiu 1984 and references therein), so we feel that such a choice for the A coefficient introduced no serious error.

There is no theoretical result concerning the processes studied in this work, i.e. the change in the fine structure state of the rubidium atom induced by collision with a K or Cs ground-state atom. Dashevskaya et al (1969a) have considered the possible mechanisms for the transfer of electronic energy in collisions between an excited alkali atom and an unexcited (dissimilar) atom and they have examined particularly the K+Rb pair. In their work, however, they have estimated the cross section for the process describing the change in the fine structure of the potassium atom. The estimated upper limit yields $\sigma < 67 \text{ \AA}^2$, while the experimental value of the cross section for this process equals 260 \AA^2 (Hrycyshyn and Krause 1969).

4. Conclusion

A diode-laser fluorescence experiment was performed in order to study fine-structure transitions between 5^2P states of a rubidium atom colliding with ground-state potassium

or caesium atoms. During the experiment the density of rubidium atoms was kept low enough for radiation trapping effects to be negligible, at least in the range acceptable for data analysis. On the other hand the densities of the perturber atoms were much larger (about 10^4 and 6×10^4 times for K and Cs, respectively) than the density of the rubidium atoms. Under these conditions the fine-structure mixing process $\text{Rb}(5^2P_{3/2}) \leftrightarrow \text{Rb}(5^2P_{1/2})$ was practically induced only by collisions with K (or Cs) and not by collisions with ground-state rubidium atoms.

In the analysis, we have used a simple three-level model (Krause 1966) which neglects the energy transfer from $\text{Rb}(^2P_{3/2})$ to $\text{K}(^2P_J)$ (or $\text{Cs}(^2P_J)$) states. Using the data of Hrycyshyn and Krause (1969b) we have estimated that, under the conditions of our experiment, the corresponding transition rates amount to less than 1% of relevant radiation transition rate A . Thus, our choice of the simple three-level model has been justified to the extent of the above mentioned correction.

As mentioned in section 3, the polarization effects in the present investigations were analysed only briefly. Taking into account these effects in more detail would certainly improve the accuracy of the presented results for the cross sections.

The obtained results cover some of the missing data for collisional energy transfer among the first resonance states in mixed alkali systems. The existing theoretical results are unsatisfactory and completeness of the set of the relevant experimental data would surely invoke the theoretical reinvestigation of these processes.

Acknowledgments

We would like to thank the Ministry of Science, Technology and Informatics (Croatia) and NIST/NBS (USA) for financial support.

References

- Ballagh R J and Cooper J 1977 *Astrophys. J.* **213** 479
Beuc R, Movre M and Vadla C 1982 *J. Phys. B: At. Mol. Phys.* **15** 1333
Czajkowski M, McGillis D A and Krause L 1966 *Can. J. Phys.* **44** 741
Czajkowski M, Skardis G and Krause L 1973 *Can. J. Phys.* **51** 334
Dashevskaya E I, Nikitin E E, Voronin A I and Zambekov A A 1969a *Can. J. Phys.* **47** 981
Dashevskaya E I, Voronin A I and Nikitin E E 1969b *Can. J. Phys.* **47** 1237
Hansen W 1984 *J. Phys. B: At. Mol. Phys.* **17** 4833
Holstein T 1947 *Phys. Rev.* **72** 1212
Hrycyshyn E S and Krause L 1969a *Can. J. Phys.* **47** 223
— 1969b *Can. J. Phys.* **47** 215
Huennekens J and Gallagher A 1983 *Phys. Rev. A* **27** 1851
Kamke B, Kamke W, Niemax K and Gallagher A 1983 *Phys. Rev. A* **28** 2254
Krause L 1966 *Appl. Opt.* **5** 1375
— 1975 *The Excited State in Chemical Physics* ed J W McGowan (New York: Wiley) pp 267–316
Movre M and Beuc R 1985 *Phys. Rev. A* **31** 2957
Ornstein M H and Zare R N 1969 *Phys. Rev.* **181** 214
Stacey V and Zare R N 1970 *Phys. Rev. A* **1** 1125
Tharangaj M A 1948 *PhD Thesis* University of Toronto
Theodosiu C E 1984 *Phys. Rev.* **30** 2881